Metallurgical and Materials Applications of
Shock-Wave and High-Strain-Rate Phenomena
L.E. Murr, K.P. Staudhammer and M.A. Meyers (Editors)

169

85

Shock induced synthesis of silicides

S. S. Batsanov[a], F. D. S. Marquis[b], and M. A. Meyers[c]

[a]Center for High Dynamic Pressures, Mendeleevo, Russia

[b]College of Chemical, Physical and Materials Science and Engineering

[c]Department of AMES, University of California/San Diego, La Jolla, CA

The conditions for initiation and propagation of reactions forming transition metal silicides from elemental powder mixtures of controlled porosity, using shock waves with a wide range of pressures (10-70 GPa) and detonation velocities, (4.2-7.4 km/s) have been investigated. Symmetrical and asymmetrical shock-wave loading experiments were conducted on elemental powder mixtures. In asymmetrical shock loading, regions of shear localization with very high plastic strains, fragmentation, interpenetration, mixing, and vortex formation were produced, which resulted in the release of considerable thermal energy. This paper discusses the concept of threshold energy for shock-induced chemical reactions and investigates the roles of shock energy, threshold energy, and energy of plastic deformation on the initiation and propagation of reaction syntheses.

1. INTRODUCTION

The synthesis of advanced materials provides the foundation of the materials science triad: manufacturing-microstructure-properties. Shock induced syntheses are very important, especially for intermetallic compounds, since their complex crystal structures make them rather intolerant to microstructural defects, and their precise stoichiometry makes the achievement of single phase microstructures rather difficult. Because of this the achievement of tailored intrinsic properties is not only rather challenging, but also critically dependent on the manufacturing processes. Shock induced synthesis of silicides offers considerable advantages, such as extremely short-term thermal exposures, with consequent minimalization of oxidation, retention of extremely fine metastable microstructures developed by dynamic processing, and formation of near net shape particles.

The propagation of shock waves through materials can generate considerable structural changes. These studies were initiated with the Manhattan Project and have been continued ever since. The first in-depth study of shock compression synthesis was conducted by Batsanov and coworkers in 1965 [1]. This was followed by work in Japan by Horiguchu and Nomura [2-5], and the Soviet Union [6-10]. In the United Sates the pioneer work of Graham, et al [11-14] was continued by Vreeland and co-workers [15-17], Horie et al. [18-19], Thadani et al. [20], Boslough [21], Thadhani et al. [22], Yu and Meyers [23], and Meyers et al. [27].

There are essentially two schools of thought regarding the onset of shock-induced chemical reactions: solid-solid vs. solid-liquid reactions. Graham [11-13] and Batsanov [9, 10, 28, 29] provide substantial evidence in favor of the former mechanism, whereas Krueger, Mutz, and Vreeland [15-17], Vecchio et al. [30], and Meyers et al. [27, 28, 30, 31] obtained results that substantiate liquid-solid reactions. Shock densification experiments conducted by Meyers et al. on powder mixtures containing Mo and Si, or Nb and Si, revealed the formation of localized reaction regions in narrow bands produced by shear localization [27, 38]. Experiments also showed that plastic deformation influenced the reaction between elemental Nb and Si powders [Yu et al. [49]]. Under shock and shear, in conditions of pressure which would not ordinarily result in reaction, localized regions in which the powder mixture had been intensely plastically deformed underwent chemical reactions. Nesterenko et al. [40] carried out controlled shear experiments, in the absence of shock compression, and demonstrated that reaction could take place.

One of the major unresolved problems in shock synthesis of hard and brittle materials is the cracking of the compacts on both the microscopic and macroscopic scales. This is because micro and macro-cracking can result from reflection components of the initial shock wave; this reflection can result from any interface in the region surrounding the powder compact. These reflected waves usually generate tensile stresses within the material, with consequent micro and macro crack formation. Another significant challenge is the development of appropriate microstructures at the macroscopic scale. In order to overcome these challenges, a better understanding of the processes of initiation, propagation and extinction of the reaction synthesis, its mechanisms and the roles played by the various energies must be achieved. This is the objective of this investigation.

2. EXPERIMENTAL PROCEDURES

Elemental Nb, Mo, and Si powders were mixed in the stoichiometric proportions $NbSi_2$ and $MoSi_2$ and were loaded into tubular steel capsules and compacted to an initial density of 70% of their theoretical values. Typical capsules had external diameters of 14 mm, lengths of 80 mm, and wall thicknesses of 2 mm and 3 mm for lower pressure and higher pressure experiments, respectively. The capsules were placed in explosive containers. The explosion was initiated at the top and the detonation wave traveled downwards, with a detonation velocity U_D, generating high pressures in the capsules. Details of the experimental procedures are provided elsewhere [27, 29]. The explosives used and the pressures generated are characterized in table 1. The pressures in the Mach Stem region were approximately seven times the pressure in the periphery.

Table 1. Characterization of explosives.

Properties & Pressures Generated	Type of Explosive		
	IIBB-4	RDX	Ammonit
ρ, g/cm^3	1.45	1.00	1.10
U_D, km/s	7.40	6.20	4.40
γ, Isentropic constant	2.97	2.66	2.87
P, GPa (Nb+2Si)			
Periphery	10.30	5.90	3.80
Mach Stem	68.90	43.80	17.60
P, GPa (Mo+2Si)			
Periphery	10.50	6.00	3.90
Mach Stem	70.40	44.90	18.20

Specimens were observed by Scanning Electron Microscopy (SEM), with the backscattering electron mode in order to differentiate the phases formed and to characterize the microstructures

obtained. Thus, the light phase is Mo or Nb, the dark phase is Si, and the grey phases are intermetallic compounds, most frequently disilicides. In addition, Energy Dispersive Spectroscopy (EDS) was used in order to determine the chemical composition and stoichiometry of the phases synthesized.

3. RESULTS AND DISCUSSION

3.1. Symmetrical Shock Loading (SSL)

Experiments were conducted with three detonation velocities: 7.4, 6.2, and 4.4 km/s. However, reaction synthesis was observed only in the first case, which is presented here. Both the Mo+2Si and Nb+2Si systems exhibited unreacted, partially reacted, and fully reacted regions. Figure 1 shows a typical macroscopic view of the cross-sections for the Mo+2Si system. These regions are marked U, P, R, respectively.

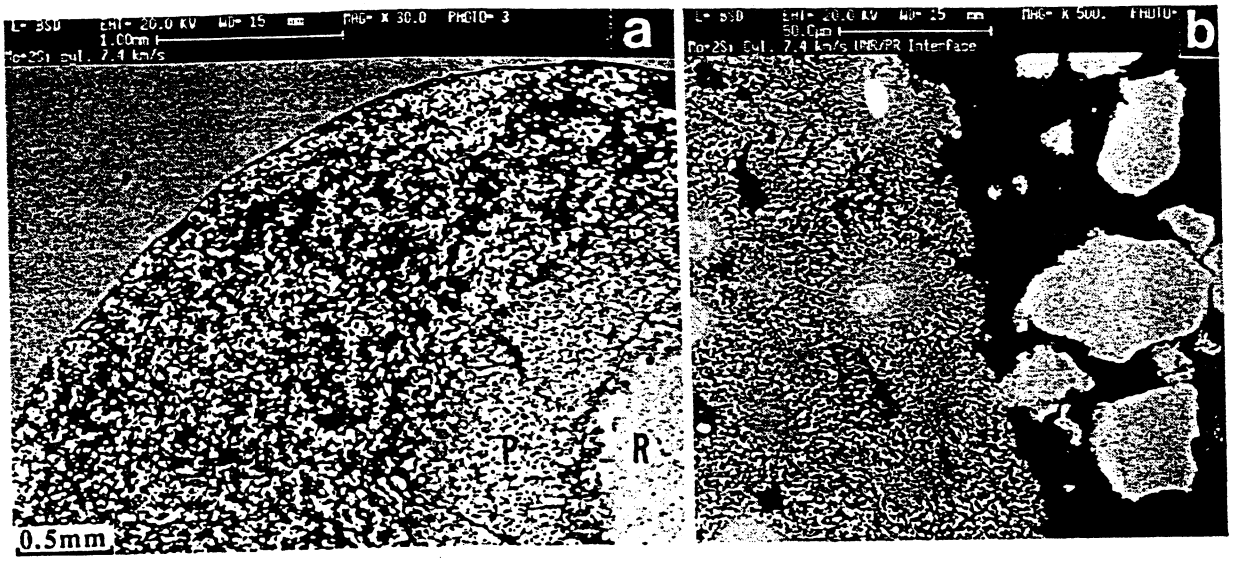

Figure 1. a) Cross-section of Mo+2Si for SSL, b) Sharp U/P interface.

There is a clear boundary between them, as shown in more detail in figure 1(b). The central Mach

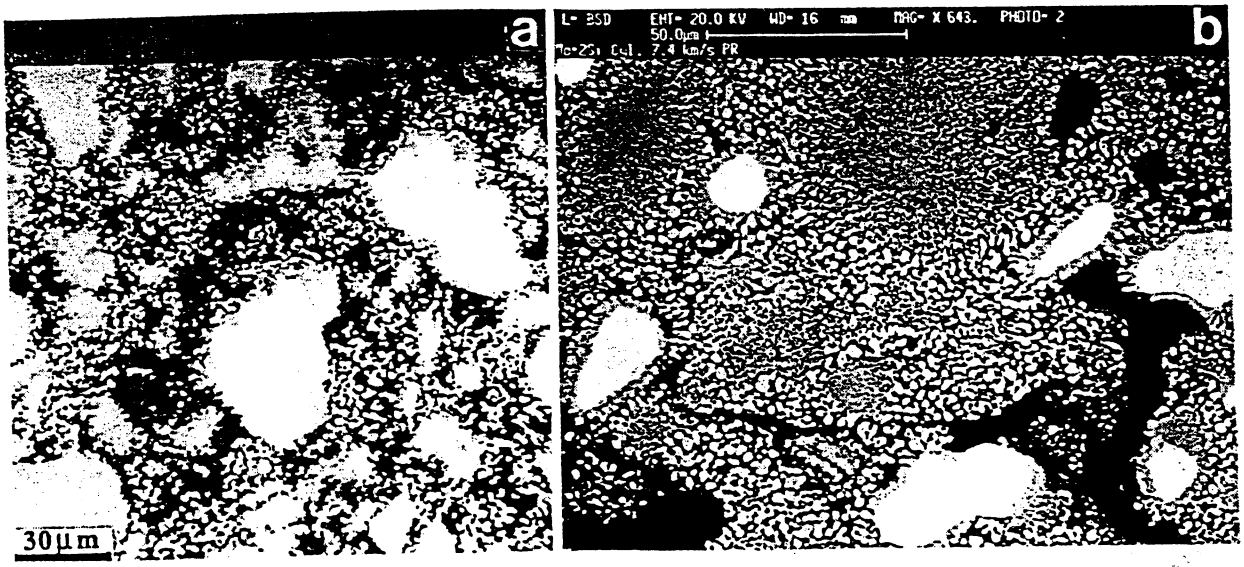

Figure 2. Partially reacted region on SSL: a) Nb+2Si, b) Mo+2Si

Stem corresponds to the fully reacted region. The partially reacted region is characterized by theformation of $NbSi_2$ and $MoSi_2$ spheroids, as observed first by Yu and Meyers [44] and described in detail elsewhere [27, 30, 31]. These spheroids have diameters of 0.5-2 μm and are larger in the periphery of Mo and Nb particles, as shown in figure 2. As the Mo and Nb particles are consumed, the diameters of the spheroids decrease. The gradation of spheroid size is seen in the totally consumed particles of figure 2. Closer to the cylinder axis, a fully reacted region was observed, as shown in figure 3. The presence of profuse spheroidal voids is an indication of complete reaction. Two phases are seen for the Nb+2Si system. These are probably $NbSi_2$ and Nb_5Si_3. Figure 1 shows the boundary between the partially reacted and the fully reacted region for Mo+2Si. The size of the $MoSi_2$ spheroids increases gradually, as the Si phase is consumed.

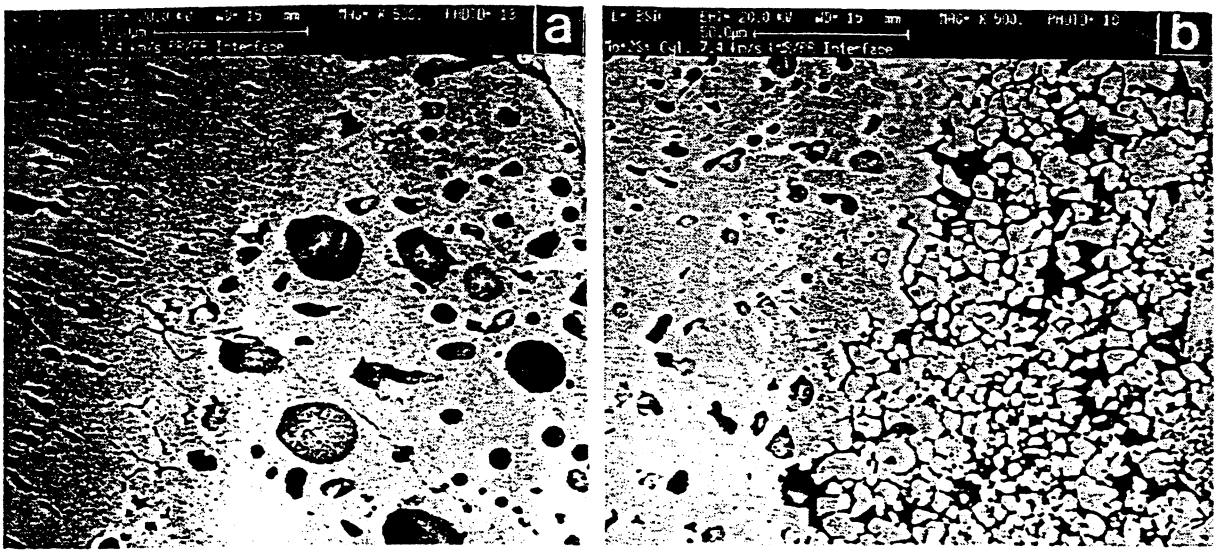

Figure 3. Interface between R and P on SSL for: a) Nb+2Si, b) Mo+2Si.

These particles become gradually more faceted. The maximum size is approximately 10 μm. The right-hand side of figure 3(a) and the left-hand side of figure 3(b) show profuse pores, complete reaction, and the separation of second lighter phase (and, therefore, richer in Mo and Nb). This phase has been identified the phase as Mo_5Si_3, which confirms the results of Vecchio et al. [30].

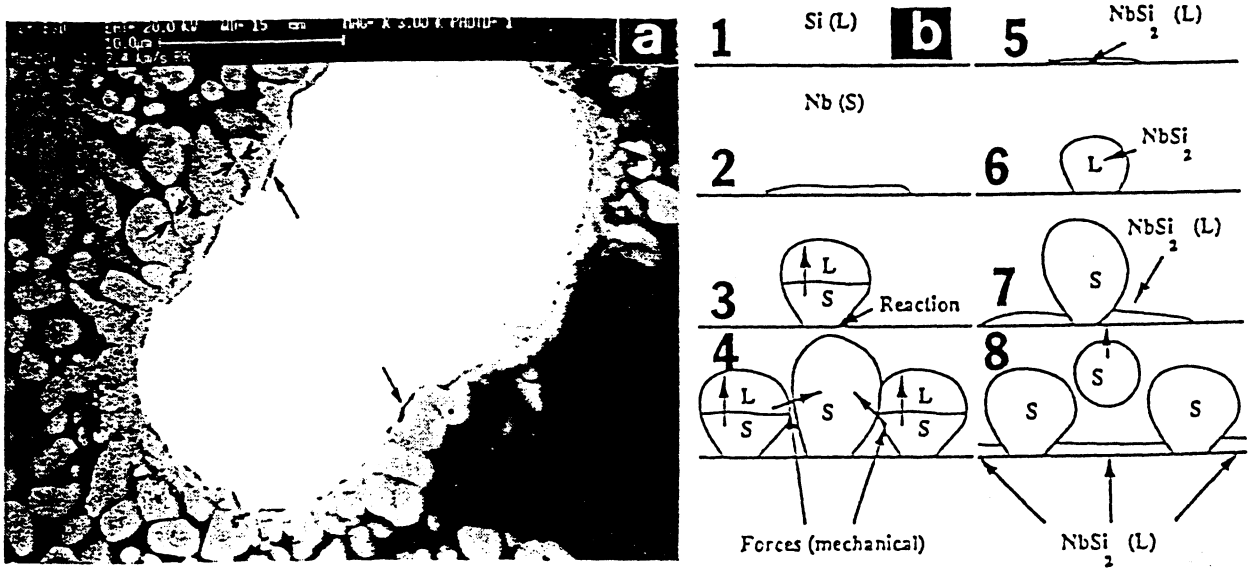

Figure 4. Synthesis mechanism, SSL for Mo+2Si: a) Cross-section, b) Schematic

The mechanism of these reactions is represented in figure 4. It is very significant that a sharp interface between U and P, and P and R, regions exists, as shown in figures 1 and 3. This means that the reaction was triggered by the shock wave, and not by thermal effects. If thermal (post shock) effects were dominant, we would observe a gradual reduction in the extent of reaction with distance from the interface. These reactions proceed according to the mechanism described first by Meyers et al., shown in figure 4 [31]. The exothermicity of the reaction is such that the products $NbSi_2$ and $MoSi_2$ are formed in the liquid state. Capillary effects lead to the formation of spheroids, in order to minimize the interfacial energy. In addition, Figure 4 shows details of the separation of the $MoSi_2$ layer from the Mo particles; these regions are marked by arrows. As the $MoSi_2$ solidifies, stresses are set up which lead to the separation of the spheroids from the Mo substrate. The spheroids subsequently move into the Si, which is molten during the reaction. The same mechanism was observed in Nb+2Si mixtures.

3.2 Modeling

The pressures and macroscopic strains generated by converging shock waves in the three loading conditions were calculated in a cylindrical reference system [27, 29, 41, 42]. Since the length of the capsules remains unchanged, $\varepsilon_z = 0$. In symmetrical shock loading the true radial and tangential macroscopic plastic strains corresponding to the porosity collapse were calculated to be $\varepsilon_r = \varepsilon_t = 0.16$, which corresponds to an effective strain $\varepsilon_e = 0.2$. In asymmetrical shock loading, an additional component of strain is present which was calculated from the dimensions a and b, assuming an elliptical distortion. Thus, the true strains were calculated to be $\varepsilon_a = -\varepsilon_b = 0.55$ which corresponds to an effective strain $\varepsilon_e = 0.64$. The deformation energy per unit of mass was calculated from the equation 1:

$$E_d = \frac{\sigma_e \, \varepsilon_e}{\rho} \tag{1}$$

where σ_e is the flow stress of the material under the imposed conditions and ρ is the material density. The flow stress of the densified Nb-Si or Mo-Si mixtures was calculated from a modified Johnson-Cook equation [45]

$$\sigma = (\sigma_0 + B\varepsilon^n)(1 + C \log \frac{\dot{\varepsilon}}{\dot{\varepsilon}_0})(1 + \frac{T^*}{T_m^*})^m \tag{2}$$

where σ_0, B, C, m, and n are parameters and T^* and T_m^* are normalized reference and melting temperatures. Ignoring work hardening and thermal softening, the equation 2 is reduced to:

$$\sigma = \sigma_0 (1 + C \log \frac{\dot{\varepsilon}}{\dot{\varepsilon}_0}) \tag{3}$$

where ε_0 is the strain rate at which the stress becomes strain rate dependent. The strain rate was calculated from the equation 4 where v is the collapse velocity of a capsule of radius r, which was estimated at v = 800 m/s [46]. Thus, the strain rate was calculated by equation $\dot{\varepsilon} = v/2r$ to be $8 \times 10^4 s^{-1}$. The compressive strengths under quasi-static conditions were estimated to be approximately 300 MPa for Nb and 90 MPa for Si [47]. The value of C, the strain-rate sensitivity, was estimated from data collected by Johnson and Cook [45]. C = 1 was found to be an average value for a number of materials. Thus from equation 3, the effective flow stress was

estimated as σ_e = 800 MPa. The deformation energy was then calculated using equation 1 for a density $\rho = 4.3 \times 10^3$ kg/m^3 and found to be E_d = 120 J/g. This value is quite low in comparison with the shock energy needed to initiate the reaction which was calculated by Meyers et al. in the 700-1,200 J/g range [30]. The Krueger-Vreeland threshold equation,

$$E_{th} = E_s = \frac{1}{2}P(V_{00} - V) \tag{4}$$

where E_{th} and E_S are the threshold and shock energies, P is the shock pressure, and V_{00} and V are the initial and shock specific volumes, respectively, was first modified by Yu et al. [43] in order to incorporate the plastic deformation energy:

$$E_t = E_s + E_d = \frac{1}{2}P(V_{00} - V) + (1 + C \log \frac{\dot{\varepsilon}}{\dot{\varepsilon}_0})\varepsilon_e \tag{5}$$

Thus, the condition for initiation would be: $E_t \geq E_{th}$. Since symmetric shock loading generated shock energies, calculated by equation 4, of 300 J/g and 190 J/g for RDX and ammonit, respectively, and the energy due to macroscopic plastic deformation is 120 J/g, the total energies calculated by equation 5 are E_t = 420 J/g and E_t = 310 J/g for detonation velocities of 6.2 and 4.4 km/s, respectively. Thus, in symmetrical shock loading, these values are still insufficient to initiate the reaction and explain our observations which show that synthesis did not occur in these cases.

3.3 Asymmetrical Shock Loading (ASL)

Asymmetrical shock loading was conducted with two detonation velocities, 4.4 and 6.2 km/s, which resulted in pressures of 3.8 and 5.9 for Nb+2Si mixtures and 3.9 and 6.0 GPa for Mo+2Si mixtures (table 1). These pressure levels were calculated to be below the critical level for

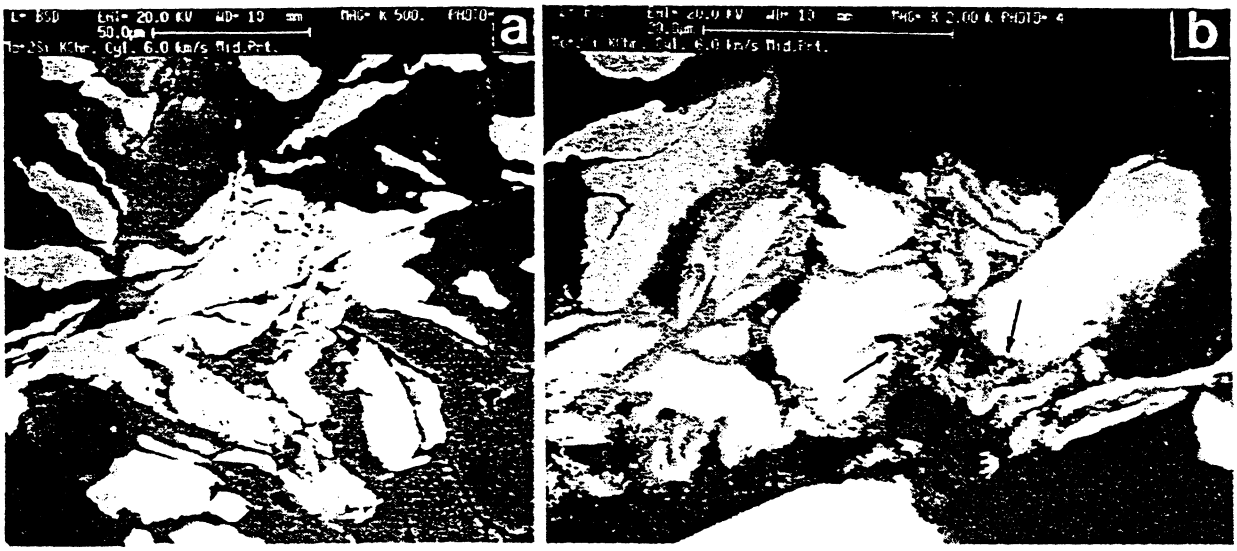

Figure 5. ASL of Mo+2Si mixtures: a) Shear band, b) Reaction mechanism.

shock induced chemical reactions, as defined by Krueger, Mutz, and Vreeland [15-17]. However, in asymmetrical shock loading the localization of plastic deformation in narrow shear bands was observed in the specimens shock compressed with a detonation velocity of 6.2 km/s

and a pressure of 6 GPa. The plastic strains within the shear-band region were estimated to be very high and to be able to exceed 10. This is confirmed by experiments carried out by Nesterenko et al. [40]. Figure 5 shows a typical area for Mo+2Si mixtures. The region within the shear-band is characterized by fracturing, interpenetration and mixing of the Nb, Mo, and Si particles and by the development of regions of considerable vortex. In this case, the energy of deformation, for a shear strain of 10, was calculated to be approximately 1,000 J/g. Since this value is of the same order of magnitude as the threshold energy, it is believed to be sufficient to trigger the reaction. This is confirmed by observation of the regions within the shear-band which exhibited clearly localized completion of the reaction, as shown by arrows in figure 5. Thus, there are two distinct mechanisms: one for SSL and the other for ASL, the later one with increased reactivity, which generates much smaller spheroidal particles, typically 0.1 to 0.3 μm in diameter, for these types of experiments.

4. CONCLUSIONS

Shock compression of Nb-Si and Mo-Si elemental powder mixtures in cylindrical capsules were specially designed to result in three regimes of pressure: a central Mach Stem with a pressure of P~70 GPa, and a peripheral area with P~10 GPa, and a transition region with P~30 GPa. The pressure was sufficient to melt the Mach Stem region with full reaction, whereas the peripheral region did not exhibit reaction. The mechanism of the reaction was by the formation of a liquid Nb-Si or Mo-Si layer surrounding the solid Nb and Mo particles, respectively. This was followed by particle spheroidization (by interfacial energy minimization), solidification, and detachment from the interface. It is demonstrated that intense localized shear deformations triggered the exothermic reaction between Nb and Si, and Mo and Si particles at shock compression pressures below the threshold value for shock-induced reactions. The Krueger-Vreeland criterion is modified to incorporate the plastic deformation energy as a component of the total energy capable of initiating the reaction. The results presented here for metal silicides indicate that shock induced synthesis can be an effective process of manufacturing of hard and brittle materials with low tolerance to microstructural defects.

ACKNOWLEDGEMENTS

This research was supported by the U.S. Army Research Office, the National Science Foundation, and the Institute for Mechanics and Materials. The help provided by S. M. Gavrilkin, H.S. Chen, and J. C. LaSalvia is gratefully acknowledged.

REFERENCES

1. S. S. Batsanov, A. A. Deribas,.E.V. Dulepov, M.G. Ermakov, and V.M. Kudinov, Combustions, Explosions and Shock Waves, 1 (1965) 47.
2. Y. Horiguchu and Y. Nomura, Carbon, 2, (1965) 436.
3. Y. Horiguchu and Y. Nomura, Chem. Inds, London (1965) 1791.
4. Y. Nomura , Less-Common Metals, 11 (1966) 378.
5. J. Horiguchi, Amer. Ceramic Soc., 49 (1966) 519.
6. G.A. Adadurov, V.I. Goldanskii, and M. Yampolskii, Chem. J., 18 (1973) 92.
7. G.A. Adadurov and V.I. Goldanskii, Russ. Chem. Revs, 50(1981) 948.
8. A.N. Dremin. and O.N. Breusov, Russ. Chem. Revs., 37 (1968) 392.
9. S.S. Batsanov, Russ. Chem. Revs., 37 (1968) 197.
10. S. S. Batsanov, G.S. Doronin, S.V. Klochdov, and A.I. Tent, Combustion, Explosion and Shock Waves, 22 (1986) 76.
11. R. Graham, B. Morosin, E.L. Venturini, and M.J. Carr, Ann. Rev. Mater. Sci, 16 (1986) 315.
12. W.F. Hammetter, R.A. Graham, B. Morosin, and Y. Horie, in Shock Waves in Condensed Matter, Elsevier Science, Amsterdam, 1988, 431.

13. R.A. Graham, Solids Under High-Pressure Shock Compression, Springer, NY, 1993.
14. B. Morosin, R.A. Graham, E.L. Venturini, M.J. Carr, and D.L. Williamson, in Shock Waves in Condensed Mattter, Elsevier Science, Amsterdam, 1988, 435.
15. B. Krueger, A. Mutz, and T. Vreeland, Mettall. Trans., 23A (1991) 55.
16. B.R. Krueger, A.M. Mutz, and T. Vreeland, J. Appl. Phys., 70(10), (1991) 5362.
17. B.R. Krueger and T. Vreeland, in Shock Wave and High-Strain-Rate Phenomena in Materials, Marcel Dekker, NY, 1992, 245.
18. Y. Horie, R.A. Graham, and I.K. Simonsen, Mater. Lett., 3 (1985) 354.
19. Y. Horie and M.J. Kipp, J. Appl. Phys., 63 (1988) 5718.
20. Z. Iqbal, N.N. Thadhani, N. Chawla, B.L. Ramakrishna, R. Sharma, S. Skumeyev, F. Reidinger, and H. Eckhardt, Appl. Phys. Lett., 55 (1989) 2339.
21. M.B. Boslough, J. Chem. Phys., 92 (1990) 1839.
22. N. N. Thadhani, A. Advani, I. Song, E.Dunbar, A. Grebe, and R.A. Graham, in Shock-Wave and High-Strain-Rate Phenomena in Materials, Marcel Dekker, NY, 1992, 271.
23. L.H. Yu and M.A. Meyers, J. Mater. Sci, 26 (1991) 601.
24. M.A. Meyers, L.H. Yu, and K.S. Vecchio, in Shock Compression of Condensed Matter-1991, North Holland, Amsterdam, 1992, 629.
25. M.A. Meyers, Scripta Metall., 12 (1978) 21.
26. M.A. Meyers, L.H. Yu, and K.S. Vecchio, Acta Metall. Mater., 42 (1994) 715.
27. M.A. Meyers, S.S. Batsanov, S.M. Gavrilkin, H.C. Chen, J.S. LaSalvia, and F.D.S. Marquis, Effect of Shock Pressure and Plastic Strain on Chemical Reactions in Nb-Si and Mo-Si Systerms, Institute for Mechanics and Materials, Report No. 94-22.
28. S.S. Batsanov, M.F. Gogulya, M.A. Bzazhnikov,E.V. Lazareva, G.S. Doronin, S.V. Klochkov, M.B. Banshikova, A.V. Fedorov, and G.V. Simakov, Sov. J. Chem. Phys., 10 (1991) 1699.
29. S.S. Batsanov, Effect of Explosions on Materials, Springer-Verlag, NY, 1994.
30. K.S. Vecchio, L.H. Yu, and M.A. Meyers, Acta Met. Mat., 42 (1994) 701.
31. M.A. Meyers, L.H. Yu, and K.S.Vecchio, Acta Met., 42 (1994) 715.
32. L.F. Vereshchagin, E.V. Zubova, and V.A. Shapochkin, Pribori, Tekhn. Esperim., 5 (1960) 89.
33. E. Teller, J. Chem. Phys., 36 (1962) 901.
34. N.S. Enikolopyan, Dokl. Akad. Nauk. SSSR, 302 (1988) 630.
35. N.S. Enikolopyan, Russ. J. Phys. Chem., 63 (1989) 1261.
36. N.S. Enikolopyan, A.A. Mkhitaryan, A.S. Karagezyan, and A.A. Khzardzhyan, Dok. Akad. Nauk. SSSR, 292 (1987) 887.
37. V.A. Zhorin, A.V. Nefed'ev, V.A. Linskii, Y.N. Novikov, R.A. Stukan, M.E. Volpin, V.I. Gold'anskii, and N.S. Enikolopyan, Dokl. Akad. Nauk. SSSR, 256 (1981) 598.
38. M.A. Meyers, Dynamic Behavior of Materials, J. Wiley, NY, 1994, 640.
39. L.H. Yu, W. Nellis, M.A. Meyers, and K.S. Vecchio, in Shock Compression of Condensed Matter-1993, Am. Inst. Physics, 1994, 1291.
40. V.F. Nesterenko, M.A. Meyers, H.C. Chen, and J.C. LaSalvia, Appl. Phys. Lett, in press, 1994.
41. R. Prummer, Explosivverdichtung Pulvriger Substanzen, Springer, Berlin, 1982.
42. M.A. Meyers and S.L. Wang, Acta Met, 36 (1988) 925.
43. J. Reaugh, J. Appl. Phys., 61(3), (1987) 962.
44. L.H. Yu and M.A. Meyers, in Shock-Wave and High-Strain-Rate Phenomena in Materials, Marcel Dekker, NY, 1992, 303.
45. G. Johnson and W. Cook, Proc. 11th Intl. Conf. on Ballistics, Netherlands.
46. A. Ferreira, M.A. Meyers, N.N. Thadhani, S.N. Chang, and J.R. Kough, Met. Trans., 22A (1991) 685.
47. H.E. Boyer and T.L. Gall, Metals Handbook, Desk Edition, ASM, 14.9, 14.10, 1985.